Generalized parton distributions of the pion in a covariant Bethe-Salpeter model and light-front models

T. Frederico[a], E. Pace[b], B. Pasquini[c] and G. Salmè[d]

[a]Dep. de Física, Instituto Tecnológico de Aeronáutica, 12.228-900 São José dos Campos, São Paulo, Brazil

[b] Dipartimento di Fisica, Università di Roma "Tor Vergata" and Istituto Nazionale di Fisica Nucleare, Sezione Tor Vergata, Via della Ricerca Scientifica 1, I-00133 Roma, Italy

[c]Dipartimento di Fisica Nucleare e Teorica, Università degli Studi di Pavia and Istituto Nazionale di Fisica Nucleare, Sezione di Pavia, Italy

[d]Istituto Nazionale di Fisica Nucleare, Sezione di Roma, P.le A. Moro 2, I-00185 Roma, Italy

The generalized parton distributions of the pion are studied within different light-front approaches for the quark-hadron and quark-photon vertices, exploring different kinematical regions in both the valence and non-valence sector. Moments of the generalized parton distributions which enter the definition of generalized form factors are also compared with recent lattice calculations.

1. Introduction

Generalized parton distributions (GPDs) represent a key concept for understanding the hadron structure [1,2,3,4,5]. They unify the information encoded in electromagnetic (e.m.) form factors (FFs) and ordinary parton distributions, supplementing them with the possibility to access new aspects of the hadron structure. In particular, the pion GPDs represent an important test ground for model calculations aiming to a detailed description of hadron structure, and this explains the wealth of papers devoted to such a task [6,7,8,9,10,11,12,13,14,15,16]. Here we review the results of Ref. [16] for the calculation of the pion GPDs in three relativistic models which explore different kinematical regions in a complementary way. In particular, the first model is a covariant analytic model, based on 4D Ansätze for the pion Bethe-Salpeter amplitude (BSA), which allows to explore the whole kinematical domain in the valence and non-valence sector. The other two models are constrained to either the valence or non-valence regions. In the non-valence region we adopt a model based on a microscopical vector-meson model dressing for the quark-photon vertex and a phenomenological Ansatz for the 3D light-front (LF) projection of the pion and vector-meson BSAs. Finally, in the valence region we discuss a third model constructed within the LF relativistic Hamiltonian dynamics.
After a short introduction about the general formalism for the definition of the pion GPDs, in Sect. 2 we present the main features of the three models, referring to [16] for a more detailed discussion. In the final section, we show the model results for the pion GPDs, together with the comparison between our model predictions and recent lattice results for the first moments of GPDs entering the definition of generalized form factors (GFFs).

2. GPDs in covariant and light-Front relativistic models

GPDs are defined as the non-forward ($p \neq p'$) matrix elements of light-cone bilocal operators separated by a light-like distance, i.e.

$$\mathcal{G}^{\Gamma} = \langle p', \pi^{\pm}| \, \mathcal{O}^{\Gamma} \, |p, \pi^{\pm}\rangle, \tag{1}$$

with

$$\mathcal{O}^{\Gamma} = \int \frac{dz^-}{4\pi} e^{ixP^+z^-} \bar{\psi}_q(-\frac{z^-}{2}, 0_\perp)\Gamma\psi_q(\frac{z^-}{2}, 0_\perp). \tag{2}$$

In Eq. (2), $P = (p + p')/2$ is the average pion momentum and the operator Γ is a matrix in the Dirac space which selects different spin polarizations of the quark fields. In particular, for $\Gamma = \gamma^+$ one has the unpolarized quark GPD H^q, while $\Gamma = i\sigma^{+i}$ projects on the transverse polarization of quarks and defines the chiral-odd GPD E^q_T. Because of Lorentz invariance the GPDs can only depend on three kinematical variables, i.e. the (average) quark longitudinal momentum fraction $x = k^+/P^+$, the invariant momentum square $t = \Delta^2 \equiv (p' - p)^2$, and the skewness parameter $\xi = -\Delta^+/(2P^+)$. In addition, there is an implicit scale dependence in the definition of GPDs corresponding to the factorization scale μ^2. The variable x allows one to single out two kinematical regions. The first region corresponds to the valence contribution and is given by the union of the interval $x \in [-1, -|\xi|]$ (for an active antiquark) and $x \in [|\xi|, 1]$ (for an active quark). In the Fock-space expansion of the pion state, this region is described by matrix elements with the same number of partons in the initial and final states. The second region corresponds to $x \in [-|\xi|, |\xi|]$, and is associated with the non-valence contribution involving non-diagonal matrix elements between parton configurations with $\Delta n = 2$.

In the forward case, $p = p'$, both Δ and ξ are zero, and H reduces to the usual parton distribution function, while E_T vanishes for time-reversal invariance.

Moments in the momentum fraction x play an important role in the theory of GPDs. Weighting Eq. (1) with integer powers of x and integrating over x, the quark operator $\mathcal{O}^{\Gamma}$ reduces to a local operator and the corresponding matrix elements can be parametrized in terms of GFFs, i.e.

$$\int_{-1}^{+1} dx\, x^{n-1} H^q(x,\xi,t) = \sum_{i=0}^{n} (2\xi)^{2i} A^q_{n,2i}(t),$$
$$\int_{-1}^{+1} dx\, x^{n-1} E^q_T(x,\xi,t) = \sum_{i=0}^{n} (2\xi)^{2i} B^q_{T\,n,2i}(t). \tag{3}$$

In Eqs. (3), the lowest moment $n = 1$ of the unpolarized GPD yields the pion e.m. FF, while the Fourier transform of $B^q_{T1,0}(t)$ in the impact-parameter space determines the dipole-like distortion of the quark density in the transverse plane due to the transverse spin-structure of the quark in the pion. The second Mellin moments of unpolarized GPDs can be related to the GFFs of the energy-momentum tensor of QCD.

The starting point of our approach is the Mandelstam formula [17] for the quark correlator in Eq. (2), giving for the u-quark unpolarized GPD

$$H^u(x,\xi,t) = -\imath\, N_c\, \mathcal{R} \int \frac{d^4k}{2(2\pi)^4} \delta(P^+x - k^+)$$
$$\times\Lambda(k - P, p')\Lambda(k - P, p)$$
$$\times Tr\left\{ S(k - P)\gamma^5 S(k + \frac{\Delta}{2})\gamma^+ S(k - \frac{\Delta}{2})\gamma^5 \right\}, \tag{4}$$

where $N_c = 3$ is the number of colors, $\mathcal{R} = 2m^2/f_\pi^2$, with f_π the pion decay constant, and m and $S(p)$ are the mass and the Dirac propagator of the constituent quark (CQ), respectively. In Eq. (4), $\gamma_5\Lambda(k,p)$ is the pion vertex function deduced from a simple effective quark-pion Lagrangian [18] . In the following, we will explore different approximations to model the momentum-dependent part of the vertex function.

In a first covariant analytic model, Λ is assumed to be a symmetric function of the two quark momenta with the following form

$$\Lambda(k - P, p) = C \frac{1}{\left[(k - \Delta/2)^2 - m_R^2 + \imath\epsilon\right]} \times \frac{1}{\left[(P - k)^2 - m_R^2 + \imath\epsilon\right]}. \tag{5}$$

A different choice, based on the sum instead of the product of the two terms in Eq. (5), was adopted in Ref. [19] for the calculation of the e.m. FF and further discussed in the case of the GPDs in Ref. [16]. However, the product form (5) provides a more realistic transverse-momentum falloff, leading to a more favourable comparison with the experimental data for the e.m. FF at

high-momentum transfer and also satisfying the support conditions for the parton distribution. Once the CQ mass is fixed and the constant C in Eq. (5) is constrained through the charge normalization, the only free parameter of the model is the regulator mass m_R, which is fitted to the experimental value of f_π. The projection into the valence and non-valence contributions to the GPDs is obtained after integration of Eq. (4) over the LF energy k^-, fully taking into account the pole structure of both the Dirac propagators and the vertex functions.

A second covariant model is introduced by following the approach of Ref. [20] for the calculation of the e.m. FFs both in the spacelike and timelike region. Starting from the same formal expression of Eq. (4) for the GPD, we introduce the following new ingredients: i) instead of the bare quark-photon vertex, γ^μ, a dressed quark-photon vertex $\Gamma^\mu(k,\Delta)$, modeled through a microscopical vector meson (VM) dominance approach, and ii) phenomenological Ansätze for the BSAs in the valence and non-valence regions. Another basic difference with respect to the previous analytic model is that only the simple analytic structure of the Dirac propagators is retained, i.e. the analytic structure is disregarded in the BSAs of both i) the initial and final pion and ii) the VM dressing of the quark-photon vertex. This approximation turns out to be a very effective one in the calculation of the e.m. FF only in the $\mathbf{\Delta}_\perp = 0$ frame [21]. which will be also adopted for the present calculation of the GPDs. In the valence sector, after integrating over the LF energy, the resulting momentum-dependent part of the 3D BSA of the pion and vector mesons are approximated with light-front wave functions (LFWFs) which are eigenstates of the CQ square mass operator of Ref. [22]. In the non-valence region, there is also a pion non-valence component describing the emission (absorption) of a pion by a quark. Assuming a vanishing pion mass, such a process can be described using a constant interaction, with a coupling constant fixed by the normalization of the pion FF. Furthermore, in the limit $m_\pi = 0$, only the pair-production mechanism is contributing to the GPD. In this term, for $m_\pi = 0$ one has only instantaneous contributions produced by the standard LF decomposition of the propagator (i.e. $S(k) = (\not{k}_{on} + m)/[k^+(k^- - k^-_{on} + \imath\epsilon)] + \gamma^+/2k^+$). In order to model the instantaneous vertex functions, we put $\Lambda^{ist} \approx \mathcal{C}\Lambda^{full}$, where the constant $\mathcal{C}$ is thought to roughly describe the effects of the short-range interactions. Indeed, we use the relative weight $\mathcal{C}_{VM}/\mathcal{C}_\pi$ as free parameter.

Finally, a third model calculation is based on a light-front Hamiltonian (LFH) approach based on a Poincarè covariant description of the pion. In particular, the rotational covariance is fulfilled through the introduction of the Melosh rotations and the proper definition of the total intrinsic angular momentum. Such a model allows us to explore only the valence region, and therefore will be discussed just for the $\xi = 0$ kinematics. In such a frame, the GPDs can be expressed as overlap of LFWFs, given by the product of the momentum-dependent part of the wave function in the initial and final state with a spin-dependent part as dictated from the proper Melosh transformations. For the momentum-dependent part we adopt a gaussian form [23], with the quark mass and the gaussian width fitted to the pion charge radius and decay constant.

3. Results

In Fig. 1 we show the unpolarized GPD H in the (x,t) plane at fixed $|\xi| = 1$, for the isoscalar $u+d$ and isovector $u-d$ quark combination, comparing the results for the covariant analytic model with a product-form for the BSA with the phenomenological BS model with dressed quark-photon vertex. The value $|\xi| = 1$ corresponds to the contribution of the pair-production mechanism in the whole range of x. The general shape for the GPDs in the two models show similar features, with the collinear peak at $x \approx 1$ increasing at higher values of $|t|$. As discussed in Ref. [16], the covariant analytic model exhibits an overall agreement also with the LFH model at $\xi = 0$, and can be used at any value of x, ξ, t for interpolating between the other two phenomenological models. In particular, at the crossing point of the valence and non-valence region, $x = |\xi|$, the covariant analytic model predicts a smooth transition, due to

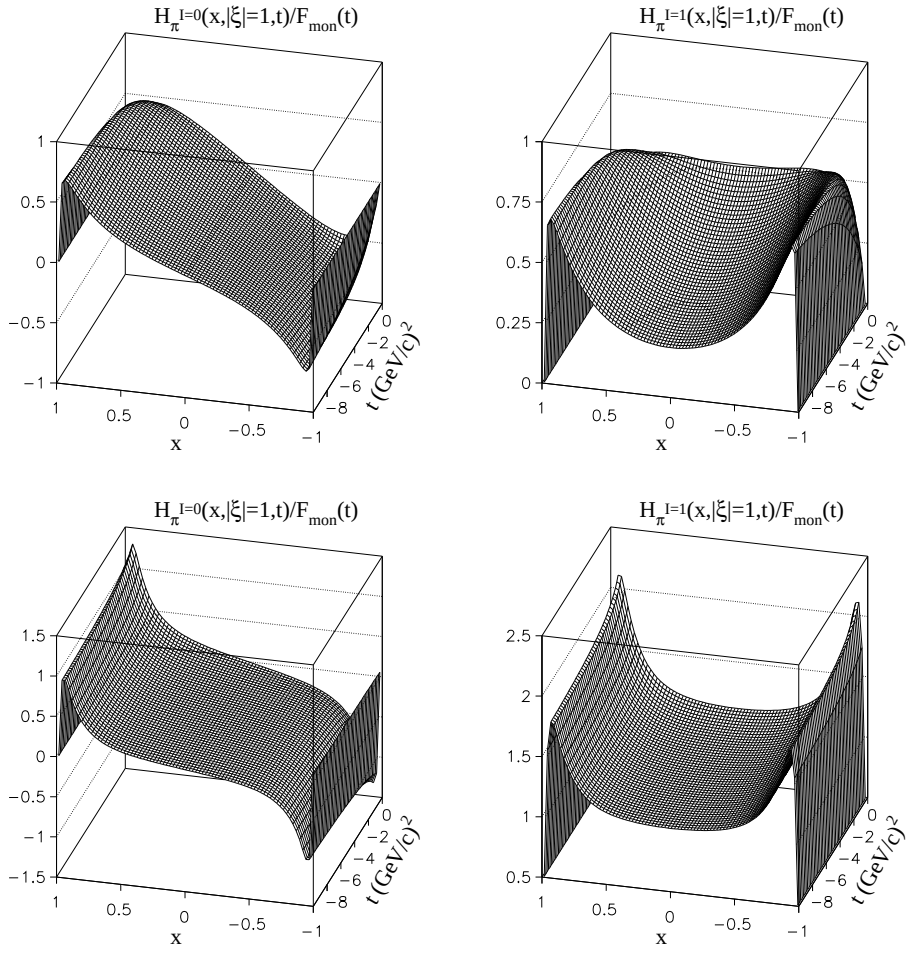

Figure 1. Upper left (right) panel: isoscalar (isovector) unpolarized GPD from the covariant analytic model with the product-form for the BSA (Eq. (5)) at $|\xi| = 1$ and $m_\pi = 0$. Lower panels: the same as in the upper panels for the microscopic model with dressed photon-quark vertex. On the z-axis the ratio with respect to $F_{mon} = 1/(1 + |t|/m_\rho^2)$ is presented. The figure is adapted from Ref. [16].

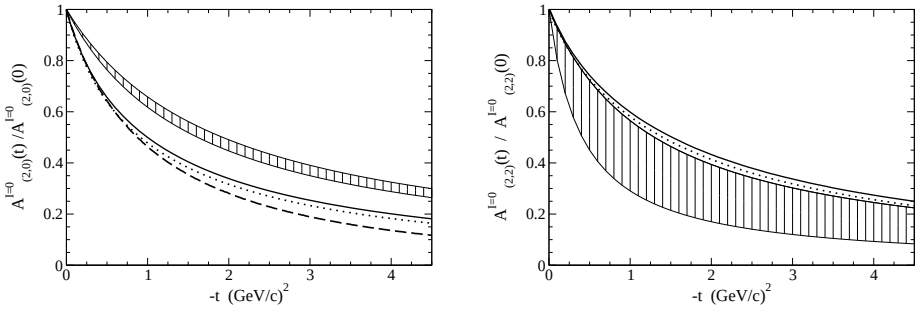

Figure 2. Left panel: the ratio $A^{I=0}_{2,0}(t)/A^{I=0}_{2,0}(0)$ as a function of t. Solid line: product-form for the pion BSA, Eq. (5), and $m_\pi = 0$. Dotted line: the same as the solid line, but with $m_\pi = 140$ MeV. Dashed line: LFH model. with a gaussian pion wave function and the proper Melosh rotations. Shaded area: results from lattice QCD [24]. Right panel: the same as the left panel, but for $A^{I=0}_{2,2}(t)/A^{I=0}_{2,2}(0)$. The figure is adapted from Ref. [16].

the continuity of the model.

In Fig. 2 we show results for the ratios of the GFFs $A^{I=0}_{2,0}(t)/A^{I=0}_{2,0}(0)$ and $A^{I=0}_{2,2}(t)/A^{I=0}_{2,2}(0)$ which are evolution-scale independent [13]. The predictions from the covariant analytic model for two different values of the pion mass are shown for both GFFs, while the LFH model can be only applied for $A^{I=0}_{2,0}(t)/A^{I=0}_{2,0}(0)$ at $\xi = 0$. The dashed band shows recent lattice results described through a monopole form $1/(1 - t/M^2_{2,i})$, as obtained in Ref. [24]. In particular, we used $M_{2,0} = 1.329 \pm 0.058$ GeV and $M_{2,2} = 0.89 \pm 0.25$ GeV, corresponding to an analysis of the lattice data that satisfies the low energy theorem, i.e. $A^{I=0}_{2,0}(0) = -4A^{I=0}_{2,2}(0)$. Our model predictions are overall consistent with the lattice results, except for small values of $|t|$. A better description of the low $|t|$ region could be obtained by incorporating in our phenomenological models interaction terms responsible for the confinement. On the other side, the large uncertainties in the lattice results for $A^{I=0}_{2,2}$ do not allow us to elaborate too much on the comparison between the different predictions.

Finally, in Fig. 3 we show the density for transversely polarized quark in the impact-parameter space $\vec{b}_\perp$. Such a density is defined as [25,26]

$$\rho^q(\vec{b}_\perp) = \frac{A^q_{1,0}(\vec{b}^2_\perp)}{2} - \frac{s^i \epsilon^{ij} b^j_\perp}{2m_\pi} \frac{\partial}{\partial b^2_\perp} B^q_{T1,0}(\vec{b}^2_\perp), \quad (6)$$

where the GFFs in the impact-parameter space are obtained by Fourier transform of Eqs. (3). In Eq. (6), the monopole distribution associated to H is distorted by a dipole term proportional to E_T in the case of transversely polarized quark. The results in Fig. 3 correspond to the LFH model and exhibit a clear correlation between quark spin and transverse space. The average sideway shift amounts to $\langle b^y_\perp \rangle^u = B^u_{T1,0}/(2m_\pi A^u_{1,0}) = 0.197$ fm. Remarkably, this value is of the same strength as the dipole-like distortion in the density of transversely polarized quarks in an unpolarized nucleon, i.e. $\langle b^y_\perp \rangle^u = B^u_{T1,0}/(2m_N A^u_{1,0}) = 0.209$ fm, as obtained in a LFH model for the nucleon [27]. These results are also supported from recent lattice calculations [26,28], giving $\langle b^y_\perp \rangle^u = 0.151(24)$ fm and $\langle b^y_\perp \rangle^u = 0.154(6)$ fm for the pion and nucleon, respectively.

Acknowledgments

This work was partially supported by the Brazilian agencies CNPq and FAPESP and by Ministero della Ricerca Scientifica e Tecnologica. It is also part of the Research Infrastructure Integrating Activity "Study of Strongly Interacting Matter" (acronym HadronPhysics2, Grant Agreement n. 227431) under the Seventh Framework Programme of the European Community.

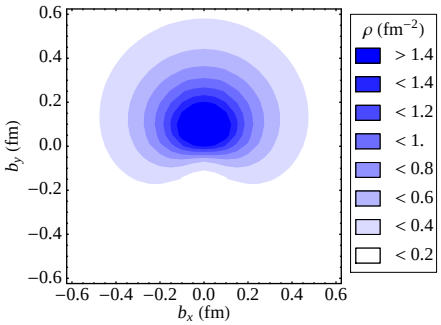

Figure 3. Density in the impact-parameter space of transversely polarized u quark in $\pi^{\pm}$ as predicted from the LFH model.

REFERENCES

1. X. Ji, Ann. Rev. Nucl. Part. Sci. 54 (2004) 413.
2. A. V. Belitsky and A. V. Radyushkin, Phys. Rept. 418 (2005) 1.
3. K. Goeke, M. V. Polyakov and M. Vanderhaeghen, Prog. Part. Nucl. Phys. 47 (2001) 401.
4. M. Diehl, Phys. Rept. 388 (2003) 41.
5. S. Boffi, B. Pasquini, Riv. Nuovo Cim. 30 (2007) 387.
6. M. V. Polyakov and C. Weiss, Phys. Rev. D 60 (1999) 114017.
7. B. C. Tiburzi and G. A. Miller, Phys. Rev. D 65 (2002) 074009; Phys. Rev. D 67 (2003) 013010; Phys. Rev. D 67 (2003) 113004.
8. A. Mukherjee, I. V. Musatov, H. C. Pauli and A. V. Radyushkin, Phys. Rev. D 67 (2003) 073014.
9. F. Bissey, J. R. Cudell, J. Cugnon, J. P. Lansberg and P. Stassart, Phys. Lett. B 587 (2004) 189.
10. L. Theussl, S. Noguera and V. Vento, Eur. Phys. J. A 20 (2004) 483.
11. M. Diehl, A. Manashov and A Schäfer, Phys. Lett. B 622 (2005) 69.
12. C.-R. Ji, Y. Mishchenko and A. Radyushkin, Phys. Rev. D 73 (2006) 114013.
13. W. Broniowski, E. R. Arriola, K. Golec-Biernat, Phys. Rev D 77 (2008) 034023; W. Broniowski and E. R. Arriola, arXiv:0901.3336 [hep-ph].
14. W. Broniowski and E. R. Arriola, Phys. Rev. D 78 (2008) 094011.
15. A. Van Dyck, T. Van Cauteren, J. Ryckebusch and B. C. Metsch, Phys. Lett. B 662 (2008) 413.
16. T. Frederico, E. Pace, B. Pasquini and G. Salmè, Phys. Rev. D 80 (2009) 054021.
17. S. Mandelstam, Proc. Royal Soc. (London) A 233 (1955) 248.
18. T. Frederico and G. A. Miller, Phys. Rev. D 45 (2002) 4207; Phys. Rev. D 50 (1994) 210.
19. J.P.B.C. de Melo, T. Frederico, E. Pace, G. Salmè, Nucl. Phys. A 707 (2002) 399.
20. J.P.B.C. de Melo, T. Frederico, E. Pace and G. Salmè, Phys. Lett. B 581 (2004) 75; Phys. Rev. D 73 (2006) 074013.
21. J.P.B.C. de Melo , T. Frederico, E. Pace, G. Salmé, J. S. Veiga, Proceedings of the Workshop on "Continuous Advances in QCD", Minneapolis (World Scientific, Singapore, 2007), p 525, and hep-ph/0609212.
22. T. Frederico, H.-C. Pauli and S.-G. Zhou, Phys. Rev. D 66 (2002) 054007; Phys. Rev. D 66 (2002) 116011.
23. P. L. Chung, F. Coester and W. N. Polyzou, Phys. Lett. B 205 (1988) 545.
24. D. Brömmel et al, [QCDSF/UKQCD Coll.] PoS(LATTICE 2007) 140; D. Brömmel, DESY-THESIS-2007-023, Jul 2007.
25. M. Diehl and Ph. Hagler, Eur. Phys. J. C **44** (2005) 87.
26. D. Brömmel et al, [QCDSF/UKQCD Coll.], Phys. Rev. Lett. 101 (2008) 122001.
27. B. Pasquini and S. Boffi, Phys. Lett. B 653 (2007) 23.
28. M. Gockeler *et al.* [QCDSF/UKQCD Coll.], Phys. Rev. Lett. 98 (2007) 222001.